JPET Fast Forward. Published on June 26, 2003 as DOI:10.1124/jpet.103.052258

Pharmacological characterization of the new stable antiarrhythmic peptide analogue ZP123: In vivo and in vitro studies.

Anne Louise Kjølbye, M.S., Carsten Boye Knudsen, Ph.D., Trine Jepsen, M.S., Bjarne Due Larsen, Ph.D., Jørgen Søberg Petersen, M.D., Ph.D., D.Sc.

Department of Pharmacology, ALK and JSP and Department of Chemistry, CBK, TJ and BDL, Zealand Pharma A/S

A) RUNNING TITLE

In vivo and in vitro studies of the new AAP analogue ZP123

B) CORRESPONDING AUTHOR:

Anne Louise Kjølbye
Zealand Pharma A/S
Smedeland 26B
DK-2600 Denmark
Phone: +45 43 28 12 24
Fax: +45 43 28 12 12
E-mail: alk@zp.dk

C)

Number of text pages: 24
Number of tables: 3
Number of figures: 6
Number of references: 19
Number of words in *Abstract*: 244
Number of words in *Introduction*: 531
Number of words in *Discussion*: 1339

D) ABBREVIATIONS

α	Rate constant associated with the distribution phase
AAPs	Antiarrhythmic peptides
AUC	Area under the plasma concentration *vs.* time curve
β	Rate constant associated with the elimination phase
C_{obs}	Observed plasma concentration
C_{ss}	Steady state plasma concentration
C(t)	Plasma concentration at time = t
$\hat{C}$	Predicted plasma concentration
$\hat{C}_{OLS}$	Predicted plasma concentration using ordinary least squares
Cl_b	Total body clearance
D	Dose
GJIC	Gap Junction Intercellular Communication

k_{obs}	Apparent rate constant
k_{10}	Fractional rate constant from the central compartment ⇒ out
k_{21}	Fractional rate constant from the peripheral compartment to the central compartment
$t_{½}$	Half-life

E)

Cardiovascular

JPET Fast Forward. Published on June 26, 2003 as DOI: 10.1124/jpet.103.052258
This article has not been copyedited and formatted. The final version may differ from this version.

ABSTRACT

Antiarrhythmic peptides (AAPs) are a group of compounds with antiarrhythmic properties, however, their use have been hampered by very low plasma stability. The aim of this study was to compare the *in vitro* and *in vivo* stability of our new stable AAP analogue ZP123 with the previously described AAP analogue AAP10. Moreover, the effect of the two compounds was examined in a murine *in vivo* model of ouabain-induced 2nd degree AV-block and the effect on dispersion of action potential duration (APD dispersion) was studied during hypokalemic-ischemia in isolated perfused rabbit hearts.

The *in vitro* $t_{½}$ of ZP123 in rat and human plasma was about 1,700 times longer than $t_{½}$ of AAP10. Due to rapid elimination, it was not possible to obtain an *in vivo* pharmacokinetic characterization of AAP10; however, calculations suggested that the clearance of ZP123 was at least 140 times longer than for AAP10. AAP10 and ZP123 produced a dose-dependent delay in onset of ouabain-induced AV-block in mice at doses of 10^{-11} to 10^{-7} mol/kg i.v. of ZP123 and 10^{-11} to 10^{-6} mol/kg i.v. of AAP10. Maximal efficacy of ZP123 was reached at a 10-fold lower dose (10^{-8} mol/kg i.v.) than with AAP10. In the isolated rabbit hearts, ZP123 and AAP10 had no effect on dispersion during control conditions. The increased APD dispersion during hypokalemic ischemia is considered a major arrhythmic substrate and only ZP123 prevented the increase in APD dispersion. In conclusion, ZP123 is a new potent AAP analogue with improved stability.

INTRODUCTION

In spite of many years of research and the availability of a wide selection of antiarrhythmic drugs, ventricular tachyarrhythmias (VT) are still a major clinical problem and one of the leading causes of death in the Western world. Especially the attempts to prevent VT by pharmacological intervention in patients recovering from myocardial infarction have been disappointing. In this patient group, most antiarrhythmic drugs are at best without impact on overall mortality (Naccarelli et al., 2000) while others may even increase mortality due to their pro-arrhythmic potential (Echt et al., 1991;Waldo et al., 1996). Only a few antiarrhythmic drugs have been shown to actually increase long-term survival in these patients (Hjalmarson, 1984;ISIS-1, 1986). Thus, there is still a great need for new, safe and effective antiarrhythmic drugs.

A group of peptides with antiarrhythmic properties (named the antiarrhythmic peptides (AAPs)) were discovered in the early eighties (Aonuma et al., 1980). The endogenous AAP (H-Gly-Pro-4Hyp-Gly-Ala-Gly-OH) was first isolated from bovine atria and was found to synchronize spontaneous automaticity of isolated cardiac myocytes (Aonuma et al., 1982). Later, several synthetic derivatives of AAP have been synthesised and tested for anti-arrhythmic efficacy *in vivo* and *in vitro* (Dhein et al., 1994;Dikshit et al., 1988;Kohama et al., 1987;Kohama et al., 1988). Among these, AAP10 (H-Gly-Ala-Gly-4Hyp-Pro-Tyr-NH_2) is one of the most potent and also the most thoroughly investigated (Dhein et al., 1994). Double cell voltage clamp studies have shown that AAP10 increases gap junction intercellular communication (GJIC) in the absence of changes in membrane conductance or basal current (Muller et al., 1997b;Muller et al., 1997a). AAPs have been shown to reduce

the increased dispersion of action potential duration during regional ischemia in isolated rabbit hearts without effects on effective refractory period (ERP) or action potential duration and shape (Dhein et al., 1994;Kjølbye et al., 2002). In addition, *in vivo* studies in rodents have demonstrated that AAPs may antagonize $CaCl_2$-, ouabain and aconitine-induced arrhythmias (Kohama et al., 1987;Kohama et al., 1988;Ronsberg et al., 1986).

By selectively acting on GJIC, the AAPs distinguish themselves from most antiarrhyhtmic drugs that affect ion channels. Considering that the pro-arrhythmic potential of most antiarrhythmic drugs are linked to their ion channel modulating effect, the fact that the AAPs presumably lack effects on ion channels make these compounds interesting as new potentially safer antiarrhythmic drugs. In addition, the role for GJIC in the mechanism of arrhythmias has been increasingly recognised in recent years. However, the therapeutic potential of the AAPs have been hampered by their poor enzymatic stability. Therefore, we developed a new AAP analogue called ZP123 (Ac-D-Tyr-D-Pro-D-Hyp-Gly-D-Ala-Gly-NH_2) that, as AAP10, increases GJIC in adult cardiomyocytes (Xing et al., 2003). ZP123 is structurally closely related to AAP10 (H-Gly-Ala-Gly-4Hyp-Pro-Tyr-NH_2); however, all L-amino acids have been substituted with D-isomers, which are expected to protect against enzymatic degradation and thereby increase the stability of the peptide. In this study, we examined the hypothesis that ZP123 has increased *in vitro* stability and a prolonged half-life *in vivo* relative to AAP10. We also investigated whether the chemical modification of the peptide changed the pharmacodynamic effects of ZP123 by comparing the electrophysiological

properties of ZP123 and AAP10 in an *in* vivo model of 2nd-degree AV-block and in the isolated rabbit heart.

MATERIALS AND METHODS

All experiments were carried out in accordance with the Guide for the Care and Use of Laboratory Animals as adopted and promulgated by the U.S. National Institutes of Health.

Drugs

ZP123 as well as the TFA salt of AAP10 and internal standard ($Gly^{4,6}$(1,2-di^{13}C-^{15}N) labeled ZP123) were synthesized in-house by standard solid-phase F-moc chemistry. The compounds were identified by mass spectrometry and the purity, determined by RP-HPLC, was determined to be 99%, 97%, and 99%, respectively.

In vitro stability of ZP123 and AAP10 in rat and human plasma

Study design

One hundred µl ZP123 or AAP10 (2 mM in water) were mixed with 900 µl lithium heparin-stabilised rat plasma or human plasma in triplicate at t = 0 and incubated at 37°C under sterile conditions. 100 µl of the drug-plasma mixture were removed at appropriate intervals based on expected half-lives and degradation was stopped by precipitation of the sample with 10 µl MeCN:TFA 50:50 v/v. The sampling intervals used for ZP123 were: 0.1min, 6h30min, 22h50min, 31h5min, 46h40min, 54h, 70h42min, 78h22min, and 166h47min whereas the intervals used for AAP10 were: 0.1, 1, 2, 3, 5, 7, 10, 15, and 20 min. A control plasma sample without the drug but treated in the

same manner was also analysed. The precipitated plasma samples were centrifuged for 15 min at 12,000 rpm at ambient temperature. The concentration of ZP123 or AAP10 was determined by RP-HPLC analysis of the resulting supernatant.

HPLC Analysis

Samples containing ZP123 and AAP10 were analysed by RP-HPLC method 1 and 2 (Table 1), respectively, using 10 µl injections.

Half-lives (t½) for the test compounds in plasma solutions were calculated from plots of the natural logarithm of the residual concentration (peak heights) against time using the formula $t½ = 1/k_{obs} \cdot \ln(2)$, where k_{obs} is the apparent first-order rate constant for the observed degradation.

Pharmacokinetics of ZP123 and AAP10 after i.v. infusion in conscious rats

Sixteen male Sprague-Dawley rats (324 - 413 g) from M&B (Denmark) were anaesthetised with a s.c. injection of Hypnorm®-midazolam solution (0.2 ml/100 g). The neurolept anaesthetic solution was prepared by mixing one part of Hypnorm® (fentanyl citrate 0.315 mg/ml and fluanisone 10 mg/ml), (Janssen) with two parts of MQW and one part of Midazolam (5 mg/ml), (Dumex-Alpharma). Catheters were inserted into the femoral vein and artery. After surgery, the rats were allowed to recover for five days before drug administration was initiated.

For the first experiment (n=8), ZP123 and AAP10, were dissolved in PBS (pH 7.4), mixed and co-administered by i.v. infusion at a rate of 25 µl/min/rat for 30 min. The average infusion rates of ZP123 and AAP10 were 8.8 and 4.4 nmol/min/kg, respectively. Prior to the experiment start the animals received an i.v. bolus dose of 500 IU heparin. The first blood sample was obtained from the artery catheter 10 min prior to infusion start and the following samples were obtained at t = 15, 29 (just before infusion stop), 32, 35, 40, 45, 55, 70, 90, 120, 150, and, 180 min. Blood samples were immediately transferred to ice chilled EDTA coated micro centrifuge tubes containing 30 µl protease inhibitor cocktail (Complete™, Roche, Germany, 1 tablet in 2 ml water). The tubes were stored on ice until centrifugation at 4 °C for 5 min (10.000 x g). The plasma (150 - 250 µl) was collected and stored at –20 °C until analysis.

In the second experiment (n=7), AAP10 dissolved in PBS (pH 7.4) was infused at a dose of 48 nmol/min/kg for 5 min, blood samples were obtained at 3 and 5 min and treated as described above.

Quantification of ZP123 and AAP10 in rat plasma

The plasma samples were thawed on ice and 170 µl plasma was diluted to 800 µl by addition of a solution containing internal standard (IS) (100 nM) and 4% (w/v) sucrose in water. For samples containing less than 170 µl plasma, the missing volume was replaced with 4% (w/v) sucrose in water.

AAP10, ZP123 and the I.S. were extracted on Waters Oasis HLB solid phase extraction columns (1 ml, 30 mg resin). Samples (600 µl) were added

to the SPE columns preconditioned with MeOH and water (1 ml of each). The columns were washed with 2% (w/v) sucrose followed by water (1 ml of each) and finally the analytes were eluted with 1 ml of 30% (v/v) MeOH in water. Following elution, samples were evaporated to dryness and reconstituted in 60 µl LC/MS/MS solvent A (Table 1). The extracted samples (40 µl) were analysed by LC/MS/MS using the conditions described in Table 1. The plasma concentration of ZP123 and AAP10 was quantified using an external standard curve (0.5 – 500 nM, n=7) extracted from spiked blank rat plasma treated in the same manner as the unknown samples. The correlation between log response (peak area x (IS conc./IS peak area)) and log concentration was linear ($R^2 \geq 0.995$) for both compounds. The lower limit of detection (LOD) of ZP123 and AAP10 was 0.70 nM and 2.6 nM, respectively. All LC/MS/MS settings, integration and calculations were controlled by Masslynx software, version 3.5 (Manchester, UK).

Pharmacokinetic calculations

Data was fitted to a two-compartment open model with zero order input *(Eq.*1) using the Nelder-Mead simplex algorithm. The weighting exponent (λ) was based on a graphical estimation of the error distribution in the data sets estimated from the slope (0.9) of the ln $((C_{obs}-\hat{C}_{OLS})^2)$ vs. ln $(\hat{C}_{OLS})$ plot (Gabrielson and Weiner, 2000). The final fitting was performed using $1/\hat{C}^{\lambda}$ as weighting function. Analysis of the standard residuals $((C_{obs}-\hat{C})/SE(\hat{C}))$ *vs.* time plots of the individual fits indicated the sample point at t = 32 min was associated with a high degree of uncertainty in five of the nine rats. The removal of this particular time point in these rats significantly improved the fits

based on sum of squared residuals (p<0.05, F-test). The data fitting sessions were performed in WinNonlin 3.1 (Pharsight Corp., Mountain View, CA, U.S.A.) and estimation of error distribution performed using Excel 97-SR2 (Microsoft Corp., Seattle, WA, USA). The body clearance of AAP10 was estimated from *Eq. 2* assuming steady state plasma concentration.

Eq. 1 $$C(t) = A_1(e^{-\alpha t} - e^{-\alpha t^*}) + B_1(e^{-\beta t} - e^{-\beta t^*})$$

where $$A_1 = \frac{D}{t_i \times V_1} \times \frac{(k_{21} - \alpha)}{(\alpha - \beta) \times \alpha} \quad \textit{and} \quad B_1 = \frac{-D}{t_i \times V_1} \times \frac{(k_{21} - \beta)}{(\alpha - \beta) \times \beta}$$

t_i= length of infusion

$t^*=t-t_i$, for $t> t_i$ and

$t^*=0$, for $t \leq t_i$

Eq.2 $$C_{ss} = \frac{R_{in}}{Cl_b}$$

where *R_{in}= infusion rate and*

C_{ss}= the plasma concentration in steady state

Effect of ZP123 and AAP10 on ouabain-induced 2nd-degree AV block in anaesthetized mice

One hundred male NMRI mice (25-30 g) from Bomholdtgaard, Ll. Skendsved, Denmark were anaesthetised by a s.c. injection of 50 – 75 µl/10 gram mouse Hypnorm®-midazolam solution. An i.v. cannula was inserted into the tail vein for i.v. administration of ouabain and another i.v. cannula was inserted for i.v. administration of vehicle, ZP123 or AAP10 (10^{-12} – 10^{-6} mol/kg i.v., n=4-12 per dose level). The lead II ECG signal was recorded continuously

by positioning of stainless steel ECG electrodes on the right forelimb and on the left hind limb. The ground electrode was placed on the right hind limb. The signal was amplified (x 5.000–10.000) and filtered (0.1-150 Hz) via a Hugo Sachs Electronic model 689 ECG module (March-Hugstetten, Germany). The analogue signal was digitised via a 12-bit data acquisition board and sampled at 1000 Hz using the Notocord HEM 3.1 software for Windows NT (Croissy-sur-Seine, France).

After a 10-min equilibration period, the test sample of drug was injected into the tail vein and three minutes later i.v. infusion of ouabain (4 mg/kg/min; ouabain, Sigma-Aldrich, Denmark) was started. Mice pre-treated with vehicle (isotonic saline) were tested on all days of the experiment as a measure of the control level in untreated animals. Injection volume was 100 µl in all experiments. The time lag to onset of AV-nodal conduction block was determined as the time from the start of ouabain infusion until the first 2^{nd}-degree AV-block. To examine the effect of test compounds on ouabain-induced changes in RR, PQ, QRS, QT intervals and T-wave height, these ECG parameters were recorded at 0, 60, 120 and 180 seconds after start of ouabain infusion. Eventually, mice developed ventricular fibrillation after about 5 minutes of ouabain infusion; this time lag was also recorded.

Effects of ZP123 and AAP10 in the isolated rabbit heart

Anaesthesia and Surgery

Male Ssc:CPH rabbits (2.5 - 4.0 kg) from Hvidesten, Denmark were anaesthetized with Hypnorm®- Dormicum®, heparinized, tracheotomized and

ventilated as previously described (Kjølbye et al., 2002). The abdominal and thoracic cavity was opened, the ascending aorta was exposed and cannulated and the heart was excised and transferred to the perfusion apparatus as previously described (the only deviation from referenced method being that the heart was not cooled with cold Krebs-Henseleit before cannulation) (Kjølbye et al., 2002).

Preparation for electrophysiological and hemodynamic recordings

After transfer to the perfusion apparatus, ECG-electrodes were positioned and a fluid filled balloon was inserted into the left ventricle for measurements of left ventricular pressure (LVP) (Kjølbye et al., 2002). The volume of the balloon was adjusted to give an end-diastolic pressure of 5-8 mmHg. Eight monophasic action potential (MAP) electrodes were placed on the epicardial surface of the heart, three on the right ventricle and five on the left. When all electrodes were in place, the water bath was elevated to ensure that the heart was immersed in 38ºC Krebs-Henseleit solution at all times.

Perfusion technique and perfusion media

The hearts were perfused with a filtered, pre-warmed (38°C) Krebs-Henseleit solution bobbled with 95% O_2/5% CO_2 (composition (mmol/l): NaCl: 118.0, KCl: 4.7, $CaCl_2$,$2H_2O$: 2.5, KH_2PO_4: 1.2, Mg_2SO_4,$7H_2O$: 1.6, sodium pyruvate: 2.0, $NaHCO_3$: 24.9, glucose: 5.6) in the Langendorff mode at constant perfusion pressure (60 mmHg) (Kjølbye et al., 2002).

Study design of isolated heart experiments

The time schedule for the experiment was as follows:

1. 15 min of perfusion with normal Krebs-Henseleit (control period).
2. 15 min of perfusion with vehicle, 0.1 nM ZP123 or 0.1 nM AAP10 added to normal Krebs-Henseleit (normokalemic treatment period).
3. 15 min of perfusion with vehicle, 0.1 nM ZP123 or 0.1 nM AAP10 added to Krebs-Henseleit solution containing a reduced K^+ concentration (2.5 mM) (hypokalemic treatment period).
4. Induction of regional ischemia followed by 30 min of perfusion with vehicle, 0.1 nM ZP123 or 0.1 nM AAP10 added to Krebs-Henseleit solution containing a reduced K^+ concentration (2.5 mM) (hypokalemic ischaemic treatment period).

Induction of regional Ischemia

Before the beginning of the experiment a ligature was placed around a major branch of the circumflex artery supplying a large part of the left ventricle. Both ends of the ligature were passed through a small plastic tube enabling induction of ischemia by pressing the plastic tube against the heart and clamping the ends of the ligature.

Effective refractory period

The effective refractory period (ERP) was measured in the border zone of the infarction at the end of the hypokalemic ischaemic treatment period by

programmed electrical stimulation, using square wave impulses of 2 msec duration at twice diastolic threshold (coaxial stimulation electrode and stimulator type 215/I Hugo Sachs Elektronik – Harvard Appartus GmbH, March-Hugstetten, Germany). The left ventricle was paced at a basic cycle length of 300 msec. For every 10^{th} impulse an extra-stimulus was superimposed with a delay of 90 msec. The delay was increased in steps of 5 msec until the extra-stimulus elicited a response. ERP was defined as the longest delay period that failed to elicit a response.

Area at Risk of Infarction

At the end of the experiment the hearts were perfused with Evans Blue dye to evaluate the area at risk of infarction as previously described (Kjølbye et al., 2002).

Recordings and measurements

Coronary flow, left ventricular pressure (LVP), perfusion pressure, lead I of the ECG and 8 MAP recordings were continuously recorded. The ECG and MAPs were sampled at 2000 Hz, and the pressure and flow parameters at 500 Hz. The output was analysed using the Notocord HEM version 3.3 software (Notocord Systems SA, Croissy-sur-Seine, France). From these recordings the following electrophysiological parameters were measured: average APD_{90}, APD_{90} dispersion, average APD_{70}, APD_{70} dispersion and dispersion of time for MAP dV/dt max.

A total of all 8 MAP recordings as well as a selective measure of the 5 MAP recordings on the left ventricle were calculated. The parameters were

measured during stable conditions on 20 consecutive complexes at the end of each of the 4 periods. Average $APD_{90/70}$ was calculated for each complex as the average duration from dV/dt max to 90 and 70% repolarisation of the MAP measurements, and an average of the 20 complexes was calculated. Likewise, the dispersion was calculated for each complex as the standard deviation of the APD measurements, and an average of the 20 complexes was calculated. Dispersion of time for dV/dt max was measured as the time-lag between the earliest and latest dV/dt max of the 8 MAP recordings. In addition, heart rate derived from LVP, LVP dP/dt max and mean coronary flow was calculated as an average of measurements from 10 sec at the end of each period starting from the time of measurement of the electrophysiological parameters.

Statistics

Two-way classified data were analysed for interaction and main effects (time, group) using a two-way analysis of variance for repeated measures and one way classified data were analysed for main effect using a one-way analysis of variance. When overall differences were detected, a post-hoc analysis was performed using Fisher's LSD test. When multiple one-way analyses of variance were performed at different time periods among the same groups, the level of significance was reduced in accordance with Bonferroni's rule of correction for multiple comparisons. Differences were considered significant at the 0.05 level. All data are mean ± SEM.

JPET Fast Forward. Published on June 26, 2003 as DOI: 10.1124/jpet.103.052258
This article has not been copyedited and formatted. The final version may differ from this version.

RESULTS

In vitro stability of ZP123 and AAP10 in rat and human plasma

The half-life ($t_{½}$) of ZP123 in rat and human plasma was 10.3 ± 1.3 days and 14.0 ± 1.5 days whereas $t_{½}$ for AAP10 in rat and human plasma was 3.8 ± 0.1 min and 11.8 ± 1.0 min, respectively.

Pharmacokinetics of ZP123 and AAP10 after i.v. infusion in conscious rats

The plasma concentration *vs.* time profile of ZP123 after 30 min i.v. infusion based on the estimated mean pharmacokinetic parameters and the obtained plasma concentrations are illustrated in Figure 1. Just before the infusion stop (29 min) the plasma concentration reached 618 ± 18 nM. After infusion stop ZP123 was rapidly distributed causing a rapid drop in plasma concentration until it entered the elimination phase approx. 20 min after infusion stop.

The central (V_c) and the steady state (V_{ss}) distribution volumes were estimated to approx. 10% and 20% (v/w), respectively. The clearance of ZP123 was found to be 12 ml/kg/min and the terminal half-life was 16 min. A summary of selected pharmacokinetic parameters is listed in Table 2.

AAP10 was not detected after 30 min infusion at a rate of 4.4 nmol/min/kg. Using the LOD of 2.6 nM as the maximum plasma concentration and assuming steady state within the 30 min infusion period, the clearance was estimated to be 1700 ml/min/kg using *eq. 2*. The detection of AAP10 in plasma was only possible after infusion of 48 nmol/min/kg, which resulted in

mean plasma concentrations of 16 ± 1.7 nM and 21 ± 1.9 nM after infusion for 3 and 5 minutes, respectively. There was no significant difference between the values obtained at 3 and 5 min ($p>0.05$, paired t-test) suggesting that steady state was reached already at this point. The clearance calculated from the plasma concentration obtained at 5 min, assuming steady state, was 2300 ml/min/kg.

Effect of ZP123 and AAP10 on ouabain-induced 2nd-degree AV-block in anaesthetized mice

I.v. infusion of ouabain (4 mg/kg/min) produced 2nd degree AV-block (as illustrated on the ECG tracing in Figure 2) after about 2 minutes. ZP123 and AAP10 prolonged the time lag until ouabain-induced AV-block dose-dependently at doses from 10^{-11} to 10^{-7} (ZP123) and 10^{-11} to 10^{-6} (AAP10) mol/kg i.v. (Figure 3A). Maximal efficacy of ZP123 was reached at a 10-fold lower dose (10^{-8} mol/kg i.v.) than for AAP10 (10^{-7} mol/kg i.v.). Both compounds showed a bell-shaped dose-response relationship with a reduced (AAP10) or no (ZP123) effect at the highest dose (Figure 3A).

Ouabain produced an increase in RR, PQ, QRS and QT intervals and an accentuated negative T-wave with a striking resemblance to the Cohn effect seen in humans during digoxin intoxication (Figure 2). However, neither ZP123 nor AAP10 affected any of the measured EEG intervals or T-wave morphology significantly relative to responses obtained in vehicle-treated mice (data not shown).

After about 5 minutes of ouabain infusion the mice developed ventricular fibrillation, which terminated the experiment. ZP123 significantly

delayed the onset of ventricular fibrillation at 10^{-9} and 10^{-7} mol/kg i.v. and AAP10 significantly delayed the onset at 10^{-9}, 10^{-7} and 10^{-6} mol/kg i.v. However, these effects seem to be random as there was no clear dose-response relationship (Figure 3B).

Effects of ZP123 and AAP10 in the isolated rabbit heart

Area at Risk

The average area at risk of infarction was similar in all groups with an average size of 44 ± 1% of the left ventricular mass.

Hemodynamics

There was no significant overall difference in heart rate among groups (table 3). Hypokalemic ischemia produced a similar and significant decrease in LVP dP/dt max and mean coronary flow in all groups (table 3).

Action potential duration and ERP

There was no difference among groups in ERP or average $APD_{90/70}$ (table 3).

Dispersion of APD

During hypokalemic ischemia the total dispersion of APD_{90} and APD_{70} increased significantly relative to the level at control in the vehicle and AAP10-treated group, whereas there was only a slight and insignificant increase in the ZP123-treated group (Figures 4A and 5A). On the left ventricle, the

dispersion increased significantly during hypokalemic ischemia relative to the control-level in all groups (Figures 4B and 5B). During hypokalemic ischemia the total and left APD_{90} and total APD_{70} dispersion was significantly lower in the ZP123-treated group than in the vehicle group. Thus, ZP123 but not AAP10 prevented the increased dispersion caused by hypokalemic ischemia. The dispersion during normokalemic treatment was similar to the level during control in all groups, and there was no difference among groups in this period.

Dispersion of time for dV/dt max

During hypokalemic ischemia the dispersion of time for dV/dt max increased significantly in the vehicle and AAP10-treated group relative to the level during control. However, 0.1 nM ZP123 completely prevented the ischemia-induced increase in dispersion. During hypokalemic ischemia the ZP123 group was significantly different from the vehicle as well as the AAP10-treated group (Figure 6).

DISCUSSION

The present study showed that ZP123 is superior to AAP10 in terms of *in vitro* and *in vivo* stability. Thus, the *in vitro* half-life of ZP123 in plasma was more than 10 days compared to less than 15 min for AAP10. This result is not unexpected, as AAP10 consists of L-amino acids that easily undergo proteolysis, while the substitution for D-amino acids in ZP123 protects against enzymatic degradation.

Due to the ultra rapid elimination of AAP10 it was not possible to perform a full pharmacokinetic characterization of AAP10. The pharmacokinetic characterization based on 30 min infusion of ZP123 showed that the plasma concentration reached approx 80% of the C_{ss} (using Eq. 2) and declined in a biphasic manner after infusion stop. The V_{ss} of 20% (v/w) correlates to the volume of extra cellular water, whereas the V_c corresponded to the distribution volume of drugs highly bound to albumin in the plasma compartment (Rowland and Tozer, 1989).

In the first experiment, AAP10 could not be detected and based on that, total body clearance of AAP10 was estimated to be at least 1700 ml/min/kg. In the second experiment, AAP10 was measured in plasma after infusion with a very high dose of AAP10 (48 nmol/min/kg) for 5 min and clearance was estimated to be about 2300 ml/min/kg. Thus, total body clearance of AAP10 was at least 140-190 times the body clearance of ZP123 confirming that ZP123 was far more stable than AAP10 *in vivo* as well as *in vitro*.

In a murine *in vivo* model of ouabain-induced 2nd degree AV block the ZP123 dose that elicited maximal effect was 10-fold lower than the AAP10

dose eliciting maximal effect, suggesting that ZP123 is more potent than AAP10 in this *in vivo* model. The rationale for using this model is that ouabain-infusion leads to high intracellular calcium levels that in turn causes uncoupling of gap junction channels and slowed conduction that may ultimately result in conduction block. Thus, the delay in time to 2^{nd}-degree AV-block was used as an indirect measure of prevention of Ca^{2+}-induced uncoupling of gap junction channels and slowed conduction. Both compounds had a bell-shaped dose-response relationship with a supra-maximal dose range. We have observed similar bell-shaped dose-response curves for AAP10, ZP123, sotalol, amiodarone, and verapamil during $CaCl_2$-induced 2^{nd}-degree AV-block in mice (unpublished observations) suggesting that the bell-shaped dose-response curve may be a characteristic finding of high calcium-associated AV-block in mice. Although bell-shaped dose-response curves are common in excitatory tissue, the exact mechanism responsible for this phenomenon during ouabain and $CaCl_2$-induced AV-block is unknown.

Neither AAP10 nor ZP123 affected the ouabain-induced increase in RR, PQ, QT or QRS interval duration. Theoretically, a compound that increases GJIC and thereby increases conduction velocity would be expected to reduce ouabain-induced prolongation of PR and QRS intervals. The reason for lack of effect on ECG-intervals in the present study is unknown but may be related to the difficulty in obtaining accurate measurements of ECG-intervals in mice.

ZP123 and AAP10 failed to dose-dependently prevent VF in this model. Whereas increased GJIC may be expected to reduce the incidence of VF caused by reentry (i.e., by preventing slowed conductance and

unidirectional conduction block), it may have little or no effect on VF caused by focal mechanisms (i.e., increased automaticity and/or triggered activity). Since ouabain-infusion produces high intracellular calcium levels, triggered activity is the likely mechanism involved in VF in this model. In addition, reentrant VF is difficult to initiate and sustain in mice due to the small size of the heart. Therefore, assuming that ouabain-induced VF is caused by a focal mechanism, the lack of a clear effect of ZP123 and AAP10 on VF in this model may not be surprising.

In the isolated perfused rabbit heart, 0.1 nM AAP10 failed to show any effects whereas 0.1 nM ZP123 significantly prevented the increase in dispersion of action potential duration and onset during hypokalemic ischemia. The compounds were only tested at one concentration and therefore it cannot be ruled out that AAP10 may be effective at other concentrations. The relatively low concentration of 0.1 nM was chosen based on previous work showing effect of 0.1 nM of the synthetic AAP-analogue HP-5 on APD dispersion in a similar model (Kjølbye et al., 2002). Moreover, earlier studies demonstrated that 0.1 nM AAP10 reduced the dispersion of activation-recovery intervals in isolated perfused normal rabbit hearts (Dhein et al., 1994). Interestingly, the same group demonstrated a 100-fold increased sensitivity of AAP10 in guinea pig papillary muscles during hypoxia (Muller et al., 1997b). Considering that maximal effect of AAP10 was achieved at 10 nM during normal conditions (Dhein et al., 1994), and cardiac sensitivity to AAP10 is increased a 100-fold during hypoxia, 0.1 nM AAP10 was chosen for the present study.

The lack of effect of AAP10 on APD dispersion following 30 min of ischemia is in accordance with previous findings. In rabbit hearts, 10 nM AAP10 reduced the activation-recovery intervals only within the first couple of minutes after induction of regional ischemia while there was no effect after 30 min (Dhein et al., 1994). Thus, present and earlier findings consistently show a weak effect of AAP10 on dispersion during ischemia. This suggests that ZP123 reduces dispersion of action potential duration more effectively than AAP10 during regional ischemia.

Increased dispersion of action potential duration is believed to facilitate the induction of reentry VT by increasing the likelihood of unidirectional block. Therefore, by reducing dispersion, ZP123 may protect against reentry VT during myocardial ischemia. This hypothesis was confirmed in a recent study of VT-inducibility in open-chest dogs 1-4 hours after ligation of the left descending artery. The study showed that 1-70 nM ZP123 prevents unidirectional block and protects against reentry VT induced by programmed electrical stimulation (Xing et al., 2003).

ZP123 and AAP10 had no effect on average APD_{90}, average APD_{70}, ERP, area at risk, or hemodynamic parameters at any point throughout the experiment. These observations are in accordance with previous findings for these compounds and for the endogenous anti-arrhythmic peptide AAP and the synthetic derivative HP-5 (Argentieri et al., 1989;Dhein et al., 1994;Kjølbye et al., 2002;Xing et al., 2003). In isolated rabbit hearts subjected to hypokalemic ischemia-reperfusion, 0.1 nM HP-5 significantly reduced dispersion of APD_{90} without affecting average APD, heart rate, contractility, or coronary flow (Kjølbye et al., 2002). In isolated canine purkinje fibres it was

shown that AAP did not affect inotropy or any of the electrophysiological parameters measured (maximum diastolic potential, action potential amplitude, maximum rate of depolarisation and action potential duration at 50% and 95% repolarisation) (Argentieri et al., 1989). In the isolated rabbit heart, AAP10 had no effect on mean action potential duration, left ventricular end-diastolic pressure, coronary flow, QRS duration or on the PQ interval (Dhein et al., 1994). In addition, AAP10 did not affect the action potential in isolated papillary muscles from guinea pig hearts in concentrations up to 1 μM (Dhein et al., 1994). Thus, there is a large body of evidence supporting the hypothesis that the AAPs selectively increase GJIC and reduces dispersion without affecting transmembrane ion currents.

In summary, the present study showed that the new AAP analogue, ZP123 reduced MAP heterogeneity during hypokalemic ischemia at a concentration where AAP10 was without effect. Moreover, ZP123 was more potent than AAP10 in protecting against ouabain-induced 2nd degree AV-block. The increased potency of ZP123 *in vivo* may be related to increased resistance to enzymatic degradation relative to AAP10, enabling sufficient plasma levels of active compound at the time of ouabain-infusion. However, the increased enzymatic stability cannot explain the difference in effects of the two compounds seen in the isolated heart experiments since perfusion in the Langendorff mode ensures a stable and constant delivery of compound. Thus, in addition to enhancing stability, the chemical modification of ZP123 may in itself by an unknown mechanism increase potency.

The potential clinical use of the AAPs have previously been hampered by their poor enzymatic stability and very short half-life, but with the

development of this novel stable AAP analogue, the therapeutic potential of antiarrhythmic peptides can be investigated *in vivo*.

ACKNOWLEDGMENTS

The authors wish to thank Henrik Holm-Kjar, Arne Lindhart Jensen and Mette Marianne Vinge for their excellent technical assistance.

REFERENCE LIST

Aonuma S, Kohama Y, Akai K, Komiyama Y, Nakajima S, Wakabayashi M, and Makino T (1980) Studies on heart. XIX. Isolation of an atrial peptide that improves the rhythmicity of cultured myocardial cell clusters. *Chem Pharm Bull (Tokyo)* **28**:3332-3339.

Aonuma S, Kohama Y, Makino T, and Fujisawa Y (1982) Studies of heart. XXI. Amino acid sequence of antiarrhythmic peptide (AAP) isolated from atria. *J Pharmacobiodyn* **5**:40-48.

Argentieri T, Cantor E, and Wiggins JR (1989) Antiarrhythmic peptide has no direct cardiac actions. *Experientia* **45**:737-738.

Dhein S, Manicone N, Muller A, Gerwin R, Ziskoven U, Irankhahi A, Minke C, and Klaus W (1994) A new synthetic antiarrhythmic peptide reduces dispersion of epicardial activation recovery interval and diminishes alterations of epicardial activation patterns induced by regional ischemia. A mapping study. *Naunyn Schmiedebergs Arch Pharmacol* **350**:174-184.

Dikshit M, Srivastava R, Kundu B, Mathur KB, and Kar K (1988) Antiarrhythmic and antithrombotic effect of antiarrhythmic peptide and its synthetic analogues. *Indian J Exp Biol* **26** :874-876.

Echt DS, Liebson PR, Mitchell LB, Peters RW, Obias-Manno D, Barker AH, Arensberg D, Baker A, Friedman L, and Greene HL (1991) Mortality and morbidity in patients receiving encainide, flecainide, or placebo. The Cardiac Arrhythmia Suppression Trial. *N Engl J Med* **324**:781-788.

Gabrielson J and Weiner D (2000) Parameter Estimation, in *Pharmacokinetic and Pharmacodynamic Data Analysis: concepts & applications* pp 21-44, Swedish Pharmaceutical Society, Stockholm.

Hjalmarson A (1984) MIAMI study--the advantage of acute treatment with metoprolol in AMI (suspected and clear). Metoprolol In Acute Myocardial Infarction. *Cardiologia* **29**:145-156.

ISIS-1 (1986) Randomised trial of intravenous atenolol among 16 027 cases of suspected acute myocardial infarction: ISIS-1. First International Study of Infarct Survival Collaborative Group. *Lancet* **2**:57-66.

Kjølbye AL, Holstein-Rathlou NH, and Petersen JS (2002) Anti-arrhythmic peptide N-3-(4-hydroxyphenyl)propionyl Pro-Hyp-Gly-Ala- Gly-OH reduces dispersion of action potential duration during ischemia/reperfusion in rabbit hearts. *J.Cardiovasc.Pharmacol.* **40** :770-779.

Kohama Y, Kuwahara S, Yamamoto K, Okabe M, Mimura T, Fukaya C, Watanabe M, and Yokoyama K (1988) Effect of N-3-(4-hydroxyphenyl)propionyl Pro-Pro-Gly-Ala-Gly on calcium-induced arrhythmias. *Chem Pharm Bull (Tokyo)* **36**:4597-4599.

Kohama Y, Okimoto N, Mimura T, Fukaya C, Watanabe M, and Yokoyama K (1987) A new antiarrhythmic peptide, N-3-(4-hydroxyphenyl)propionyl Pro-Hyp-Gly-Ala-Gly. *Chem Pharm Bull (Tokyo)* **35**:3928-3930.

Muller A, Gottwald M, Tudyka T, Linke W, Klaus W, and Dhein S (1997a) Increase in gap junction conductance by an antiarrhythmic peptide. *Eur J Pharmacol* **327**:65-72.

Muller A, Schaefer T, Linke W, Tudyka T, Gottwald M, Klaus W, and Dhein S (1997b) Actions of the antiarrhythmic peptide AAP10 on intercellular coupling. *Naunyn Schmiedebergs Arch Pharmacol* **356**:76-82.

Naccarelli GV, Wolbrette DL, Patel HM, and Luck JC (2000) Amiodarone: clinical trials. *Curr.Opin.Cardiol.* **15**:64-72.

Ronsberg MA, Saunders TK, Chan PS, and Cervoni P (86 A.D.) The antiarrhythmic effect of antiarrhythmic peptide (Gly-Pro-4Hyp-Gly-Ala-Gly) and its analog on chemically-induced arrhythmias in mice. *Med Sci* **14**:350-351.

Rowland M and Tozer TN (1989) Small volume of distribution, in *Clinical Pharmacokinetics, concepts and applications* pp 438-450, Lea & Febiger, Philadelphia.

Waldo AL, Camm AJ, deRuyter H, Friedman PL, MacNeil DJ, Pauls JF, Pitt B, Pratt CM, Schwartz PJ, and Veltri EP (1996) Effect of d-sotalol on mortality in patients with left ventricular dysfunction after recent and remote myocardial infarction. The SWORD Investigators. Survival With Oral d-Sotalol [published erratum appears in Lancet 1996 Aug 10;348(9024):416]. *Lancet* **348**:7-12.

Xing D, Kjølbye AL, Nielsen MS, Petersen JS, Harlow KW, Holstein-Rathlou N-H, and Martins JB (2003) ZP123 Increases Gap Junctional Conductance and Prevents Reentrant Ventricular Tachycardia During Myocardial Ischemia in Open Chest Dogs. *J.Cardiovasc.Electrophysiol.* **14**:510-520.

JPET Fast Forward. Published on June 26, 2003 as DOI: 10.1124/jpet.103.052258
This article has not been copyedited and formatted. The final version may differ from this version.

FIGURE LEGENDS

Figure 1: The plasma concentration vs. time profile of ZP123 after 30 min i.v. infusion. The solid line represents the theoretical curve based on the mean parameters obtained after PK modeling (table 2) and the open circles represents the mean plasma concentrations from all rats (n=8) and the error bars indicate the standard deviation.

Figure 2: Representative tracing illustrating ouabain-induced 2nd degree AV-block (arrow) in a mouse. Please note the deep T waves during ouabain intoxication.

Figure 3: A) Effect of ZP123 and AAP10 on time to 2nd degree AV-block and **B)** Effect of ZP123 and AAP10 on time to ventricular fibrillation during i.v. infusion of ouabain 4 mg/min/kg b.w. *: $p<0.05$ *vs.* vehicle, §: $p<0.05$ *vs.* same dose of AAP10. Values are means ± SEM, n=4-12/group.

Figure 4: A) Dispersion of APD_{90} (total) and **B)** Dispersion of APD_{90} (left). §: $p<0.05$ *vs.* Control within group; *: $p<0.05$ *vs.* vehicle within period; #: $p<0.05$ *vs.* AAP10 within period. Values are means ± SEM.

Abbreviations: NTP: Normokalemic treatment period, HTP: Hypokalemic treatment period, HITP: Hypokalemic ischemic treatment period.

Figure 5: A) Dispersion of APD_{70} (total) and **B)** Dispersion of APD_{70} (left). §: $p<0.05$ *vs.* Control within group; *: $p<0.05$ *vs.* vehicle within period. Values are means ± SEM.

Abbreviations: NTP: Normokalemic treatment period, HTP: Hypokalemic treatment period, HITP: Hypokalemic ischemic treatment period.

Figure 6: A) Dispersion of time for dV/dt max (total) and **B)** Dispersion of time for dV/dt max (left). §: $p<0.05$ *vs.* Control within group; *: $p<0.05$ *vs.* vehicle within period; #: $p<0.05$ *vs.* AAP10 within period. Values are means ± SEM.

Abbreviations: NTP: Normokalemic treatment period, HTP: Hypokalemic treatment period, HITP: Hypokalemic ischemic treatment period.

Table 1: *HPLC & LC/MS/MS methods*

Parameter	HPLC method 1	HPLC method 2	LC/MS/MS
Apparatus	Agilent 1100 HPLC system with binary pump, auto sampler, column thermostat and diode array detector.		Waters Alliance HT 2790 coupled to a Micromass Quattro Ultima II triple quadrupole mass spectrometer.
Solvent A: Solvent B:	0.02% HFBA in water (v/v) 0.02% HFBA in 10:90 water:MeOH (v/v/v)	0.1% TFA in water (v/v) 0.1% TFA in 10:90 water:MeOH (v/v/v).	0.02% HFBA in 5:95 MeOH:water (v/v/v) 0.02% HFBA in 10:90 water:MeOH (v/v/v)
Column:	Luna C_{18}(2), 150x2 mm, 3 µm (30 °C) (Phenomenex, Torrance, CA, USA)	Vydac 218MS52 C_{18}, 250x2.1 mm, 5 µm (30 °C) (Vydac, Hesperia, CA, USA)	XterraMS C_{18}, 50x3 mm, 3.5 µm (50 °C) (Waters, Milford, MA, USA)
Flow rate:	0.200 mL/min	0.200 mL/min	0.200 mL/min
Gradient:	Initial: 5% B Linear gradient: 0 – 5 min, 5 to 30% B Isocratic: 5 – 15 min, 30% B Wash: 16 - 17 min, 95% B Equilibration: 18 - 35 min, 5% B	Initial: 0% B Linear gradient: 2 –14 min, 0 to 25% B Wash: 15 - 16 min, 100% B Equilibration: 17 - 30 min, 0% B	Initial: 0% B Linear gradient: 0 –4 min, 0 to 100% B Wash: 4 – 4.9 min, 100% B Equilibration: 5 - 10 min, 0% B
Detection:	UV at 214.5 nm	UV at 214.5 nm	Parent > daughter m/z, (collision energy):

			ZP123: 618.10 > 413.15 (15 V) AAP10: 576.30 > 391.30 (20 V) I.S.: 624.1 > 419.15 (15V) Collision gas: Ar (1 x 10^{-3}mbar) Capillary & Cone Voltage: 3,000 & 45 V Cone Gas (N_2): 100 L/hr (100 °C) Desolvation Gas (N_2): 600 L/hr (350 °C)

JPET Fast Forward. Published on June 26, 2003 as DOI: 10.1124/jpet.103.052258
This article has not been copyedited and formatted. The final version may differ from this version.

Table 2: *Selected pharmacokinetic parameters for ZP123 after i.v. infusion. Values are means ± SEM (n=8).*

Parameter	Unit	Mean ± SEM
Dose	nmol/kg	270 ± 7
AUC	min x nM	22,000 ± 800
Cl_b	mL/kg/min	12 ± 0.36
V_c	mL/kg	89 ± 11
V_{ss}	mL/kg	190 ± 10
$t_{½,\alpha}$	min	2.5 ± 0.43
$t_{½,\beta}$	min	16 ± 0.91
k_{10}	min^{-1}	0.15 ± 0.014

Abbreviations: AUC: area under the plasma concentration curve, Cl_b: Body clearance, V_c: central distribution volume, V_{ss} Steady state distribution volume, $t_{½,\alpha}$: half-life associated with the distribution phase, $t_{½,\beta}$: Half-life associated with the elimination phase, and k_{10}: fractional rate constant from the central compartment ⇒ out.

Table 3: *Hemodynamic and electrophysiological parameters in the isolated perfused rabbit heart*

	Vehicle (n=12)				ZP123 (0.1 nM) (n=12)				AAP10 (0.1 nM) (n=8)			
	Control	**NTP**	**HTP**	**HITP**	**Control**	**NTP**	**HTP**	**HITP**	**Control**	**NTP**	**HTP**	**HITP**
Area at risk (%)				41				44				44
Heart rate (beats/min)	156±8	158±9	148±9	142±9	164±10	173±11	148±9	137±10	168±10	181±9	133±11	120±7*
LVP dP/dt max (mmHg/s)	1563±51	1554±45	1475±68	735±68*	1424±77	1446±73	1248±69	778±79*	1445±63	1464±62	1025±96	589±70*
MCF (ml/min)	56±2	54±2	53±3	32±3*	51±2	51±2	46±2	30±3*	56±3	55±3	45±4	28±4*
APD_{90} total (msec)	117±5	117±5	129±4	132±2*	107±7	107±8	119±6	130±5*	113±7	103±5	116±5	126±4
APD_{90} left (msec)	112±5	112±5	124±4	129±4*	103±7	102±8	115±6	129±6	110±7	99±5	115±6	125±4
APD_{70} total (msec)	100±5	101±4	107±4	101±3	90±6	91±7	97±7	104±5	93±6	87±5	91±4	86±3
APD_{70} left (msec)	93±6	95±5	101±5	91±5	84±6	85±7	93±5	100±5	87±6	81±5	88±4	79±2
ERP (msec)				113				118				107

*: $p<0.05$ *vs.* Control within group. Values are means ± SEM. Abbreviations: NTP: Normokalemic treatment period, HTP: Hypokalemic treatment period, HITP: Hypokalemic ischemic treatment period. LVP: Left ventricular pressure, MCF: Mean coronary flow, APD: Action potential duration, ERP: Effective refractory period.

JPET Fast Forward. Published on June 26, 2003 as DOI: 10.1124/jpet.103.052258

Figure 1

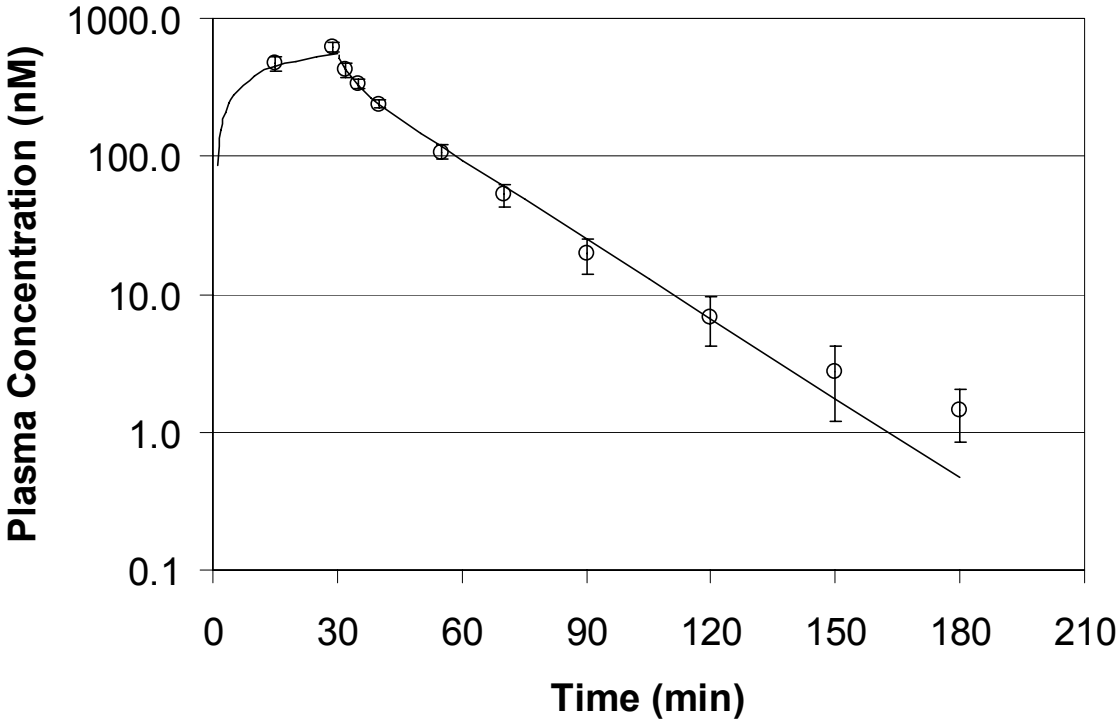

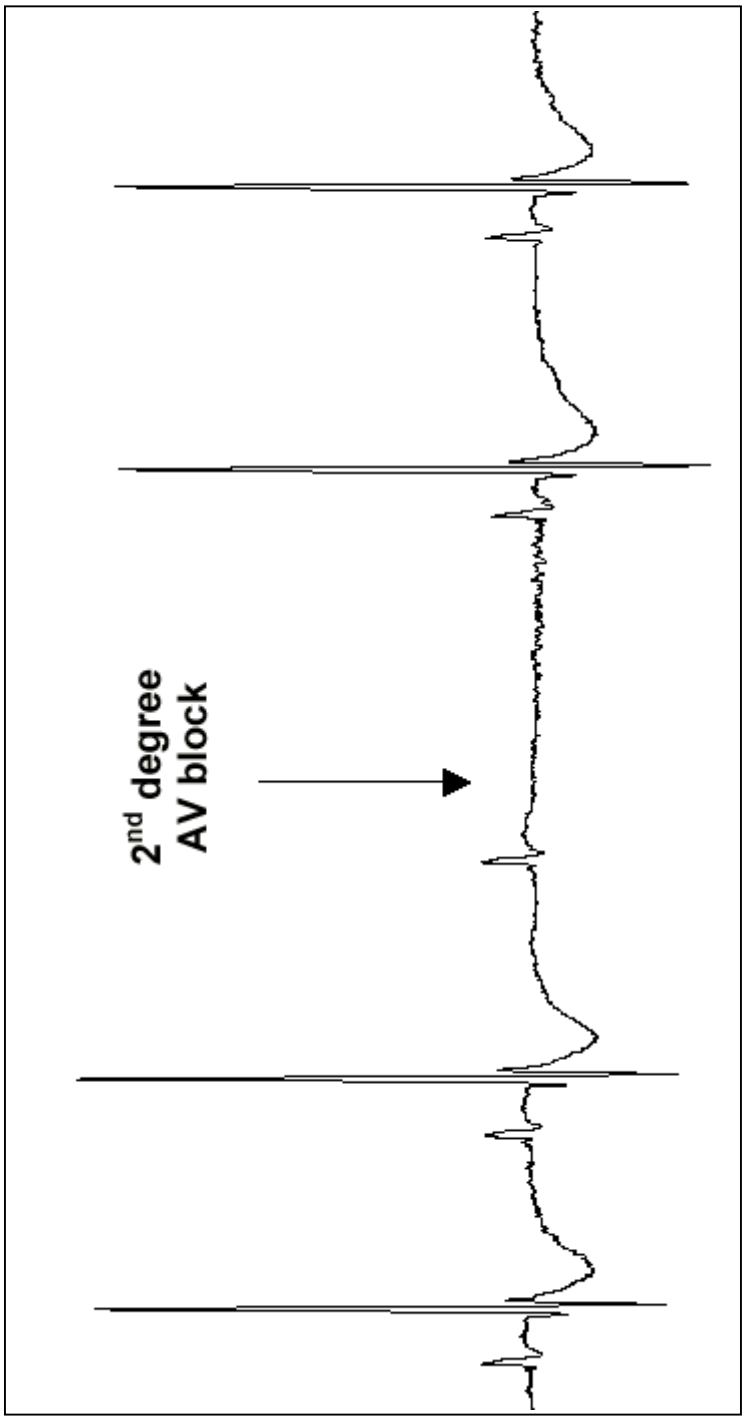

FIGURE 2

FIGURE 3

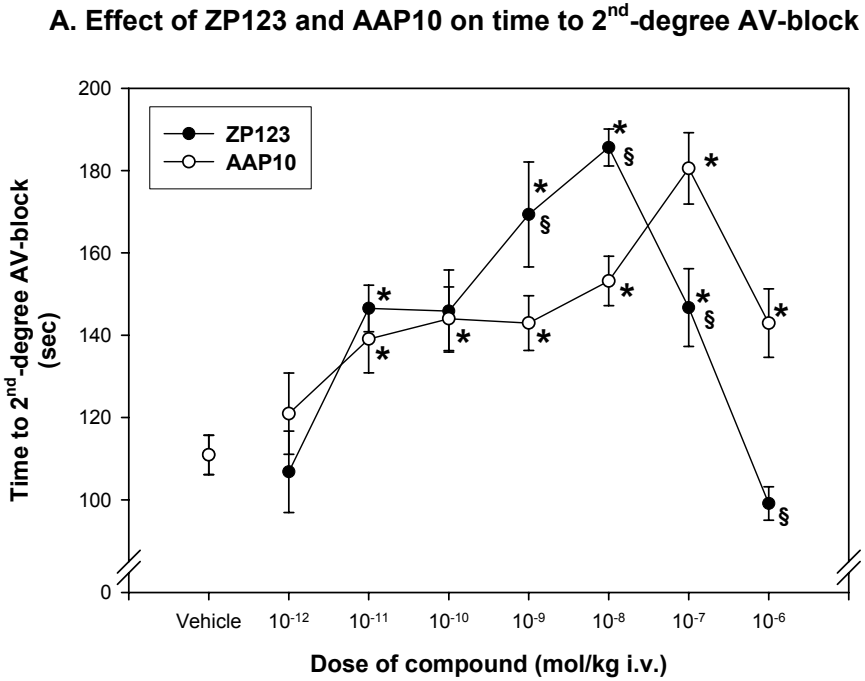

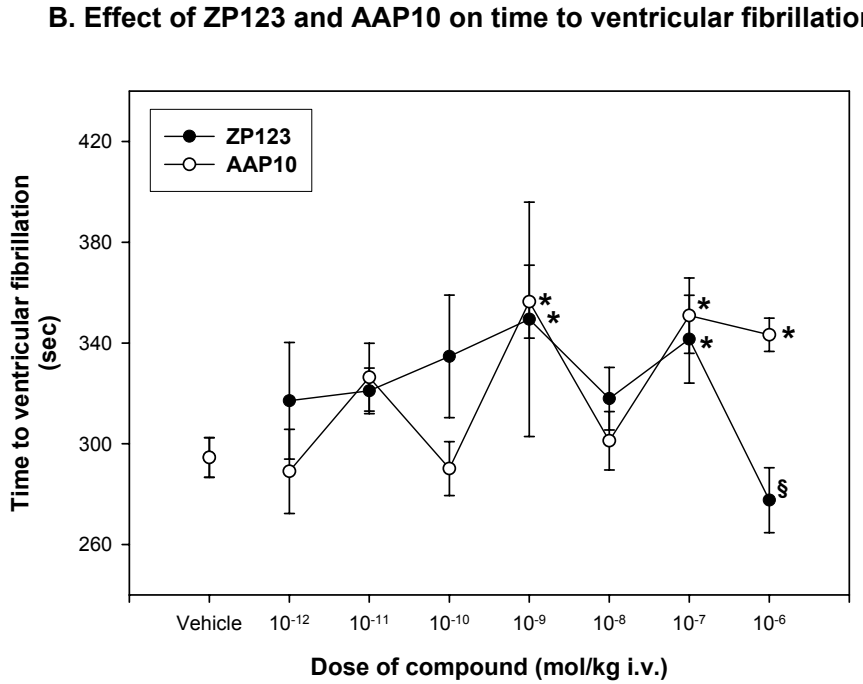

FIGURE 4

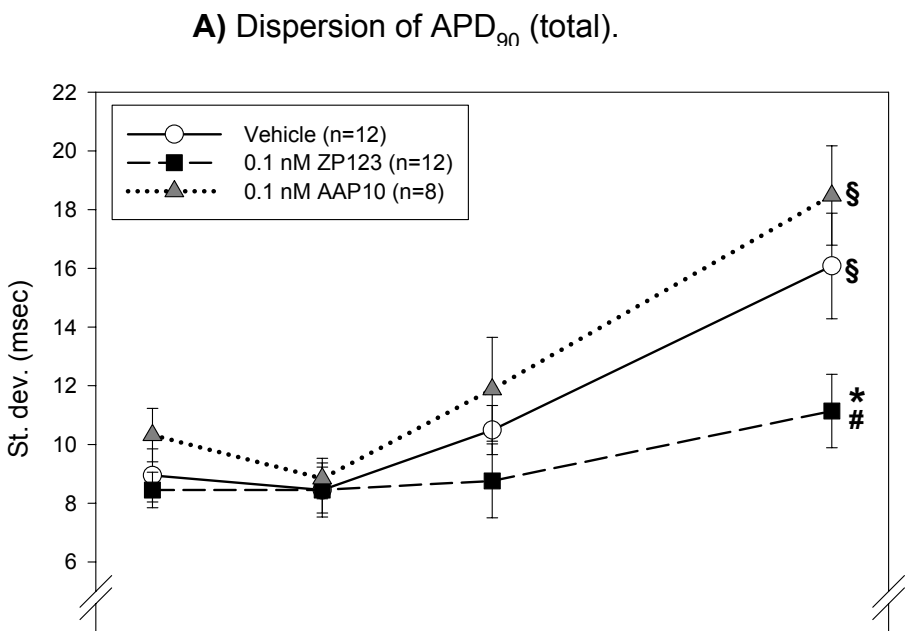

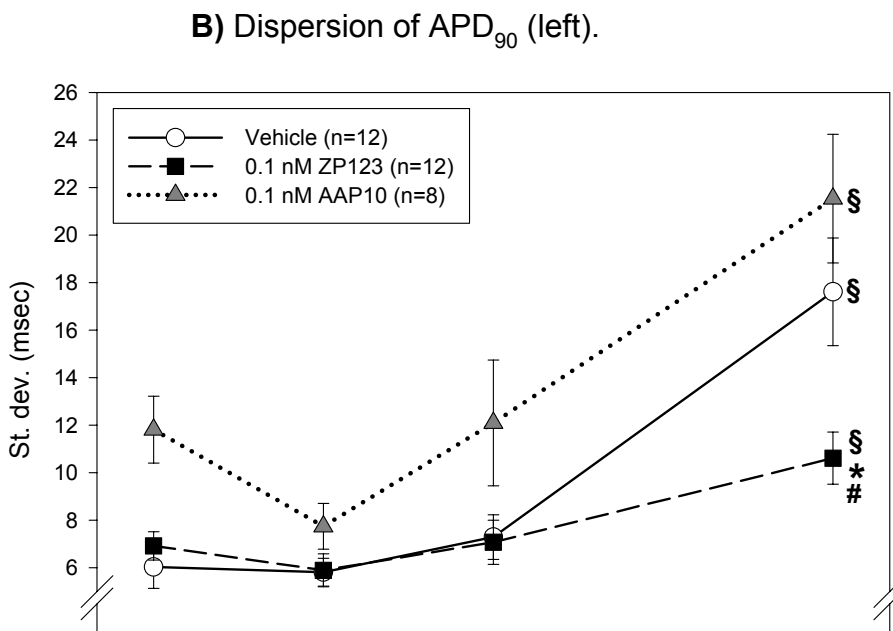

FIGURE 5

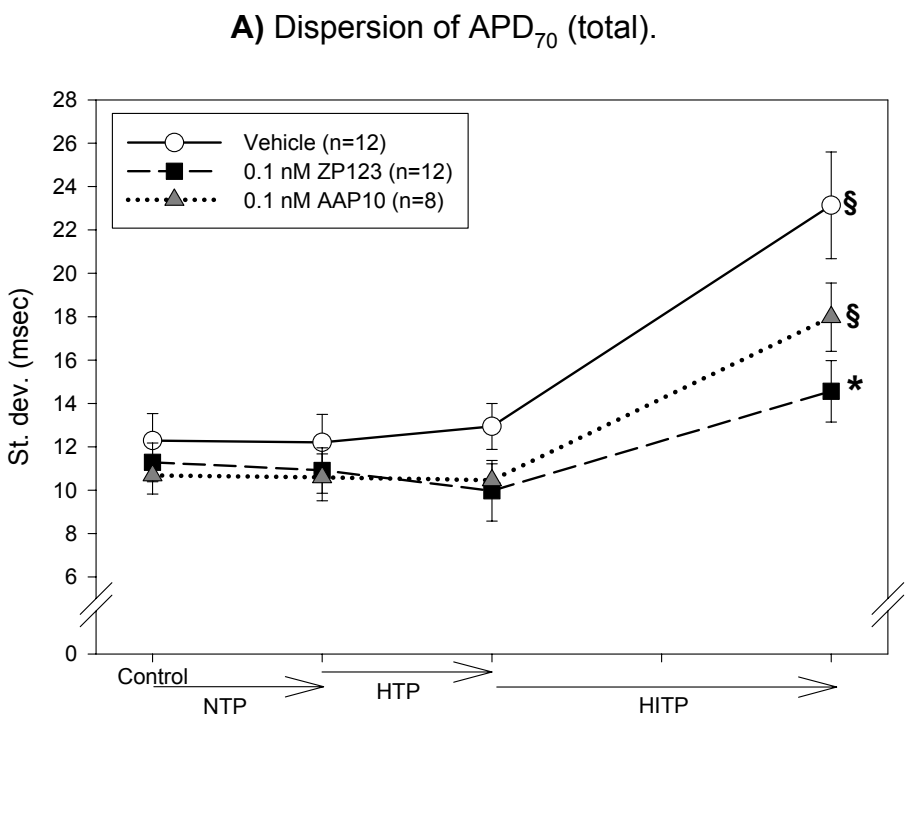

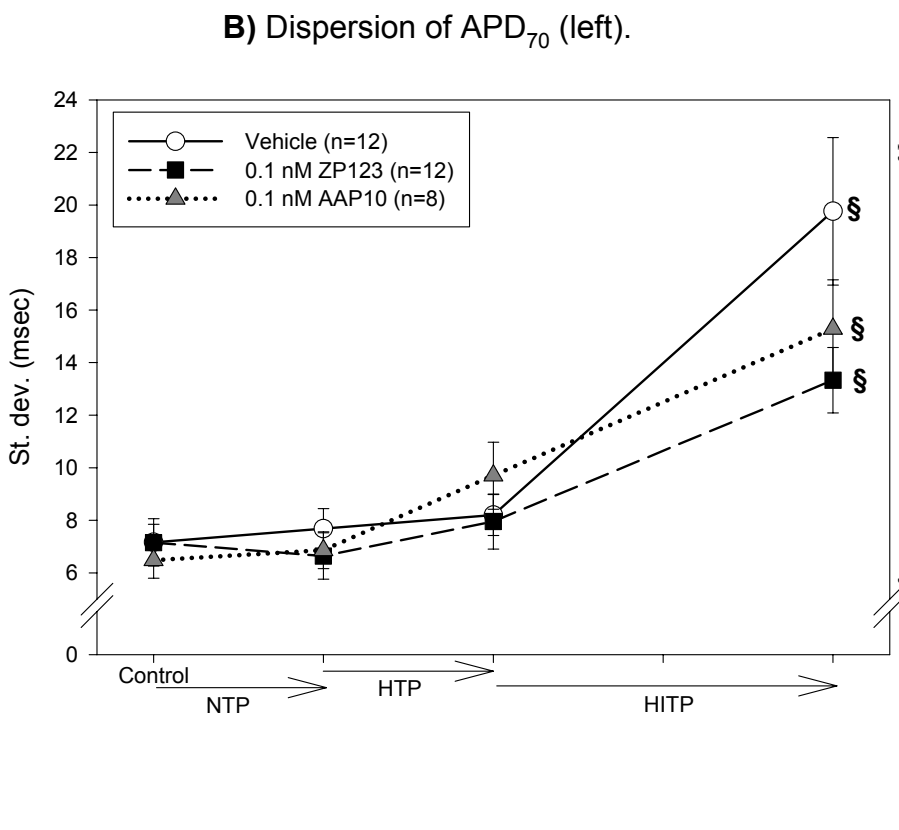

FIGURE 6